International Journal of Engineering

Journal Homepage: www.ije.ir

Fabrication of Aluminum 5083/SiC Surface Composite on Tungsten Inert Gas Weld Joint by Novel Direct Friction Stir Processing Technique

K. D. Tandel*, J. V. Menghani

Sardar Vallabhbhai National Institute of Technology, Surat, India

P A P E R I N F O

Paper history:
Received 25 November 2022
Received in revised form19 December 2022
Accepted 20 December 2022

Keywords:
Autogenous Tungsten Inert Gas Welding
Direct Friction Stir Processing
Hollow Tool
Surface Modification

A B S T R A C T

For the creation of surface reinforcement particles in the metal matrix, friction stir processing is frequently utilized. Formation of aluminum/SiC surface composite on tungsten inert gas (TIG) butt weld of Al5083 by a novel technique of direct friction stir processing (DFSP) using a hollow tool is successfully demonstrated in this work. Deposition of SiC in the stir zone of DFSP was confirmed by X-ray diffraction (XRD) method. Micro analysis of weld joint was achieved using metallographic microscope and scanning electron microscope (SEM). Microstructure of stir zone of DFSP shows finely distributed SiC reinforcement particles in aluminum matrix. Absence of detrimental intermetallics was confirmed by energy dispersive spectroscopy (EDS) analysis. Tensile strength of DFSPed specimen was found to be 227.3 MPa which is 19.5% lower than UTS of autogenous TIG weld specimen. Microhardness of SZ of DFSP was found to be increased from TIG weld microhardness of 86 Hv to 107 Hv due to presence of SiC particles.

***doi**: 10.5829/ije.2023.36.03c.12*

1. INTRODUCTION

Aluminum alloys are incredibly superior material for space, marine and automobile applications due to their specific properties like good low temperature ductility, high strength to weight ratio, good weldability and good corrosion resistance. Al 5083 is a non-heat treatable aluminum alloy having excellent sea water and industrial chemical corrosion resistance and possesses maximum strength among all non-heat treatable aluminum alloys. However, their mechanical properties like wear resistance and hardness are not very promising. The mechanical properties of Al 5083 can only be enhanced in a few ways [1].

The continuous pursuit of lightweight materials with tailored properties to meet the increasing need for energy efficient and tenable structure resulted in the creation of composite materials. Two or more components with different physical and chemical properties are combined to form a composite material. When they are united, they produce a material which is having desirable characteristics that are superior than individual components. The composite materials are unique and distinguishable in the final product [2]. One of the most extensively utilized approaches for improving the mechanical characteristics of aluminum alloys is metal matrix composite (MMC) technology, in which particles are reinforced across the entire volume. In MMCs, secondary phase reinforcements are combined with a metal matrix that is rather light. For composites to function as the primary load-bearing element, reinforcements are mostly in the form of granules, whiskers, or fibres. Ceramics, carbides, nanotubes, and oxides such as Al_2O_3, B_4C, TiC, SiO_2, TiN, SiC and carbon nanotubes are some of the most often utilized reinforcements in MMCs [3]. MMCs strengthened with ceramic particles have better strength, elasticity, and resilience to wear, fatigue, and creep than unreinforced metals, making them ideal structural materials for the automobile and aerospace sectors. Major drawback of

*Corresponding Author Email: kdtandel.gecd@gmail.com
(K. D. Tandel)

Please cite this article as: K. D. Tandel, J. V. Menghani, Fabrication of Aluminum 5083/SiC Surface Composite on Tungsten Inert Gas Weld Joint by Novel Direct Friction Stir Processing Technique, ***International Journal of Engineering, Transactions C: Aspects,*** Vol. 36, No. 03, (2023) 523-531

these composites is deterioration of ductility and impact strength because of inclusion of strong, hard to deform ceramic particles, this, to some extent, restricts their vast range of uses.

For numerous applications, where corrosion and wear resistant characteristics is required in the component, the service life of the component is mostly determined by their surface characteristics. In these cases, it is preferable to reinforce only the top layer of the material with ceramic particles, while the remaining bulk of the material keep their original structure and composition with higher ductility and toughness, referred to as surface composites (SC) [4].

Aluminum matrix composites are fabricated by numerous methods which can be broadly categorized in to liquid state, and solid state deposition process. In recent times, many surface modification techniques which calls for processing of liquid phase at elevated temperature, such as laser melt treatment [5], plasma spraying [6], high-energy electron beam irradiation [7], and casting [8], are evolved to create MMCs. In this situation, it is difficult to avert reaction between the surface reinforcement and the metal matrix and thus emergence of unfavorable brittle phases is inevitable. Above mentioned difficulty can be averted by processing SC below melting point temperature of the metal matrix. A solid state technique such as Friction Stir Processing (FSP) is the best suited to avoid reaction between reinforcement particle and metal matrix and to maintain the elemental state of the metallic particle [4]. FSP was invented and evolved by Mishra et al. [9], which works on the principle of Friction Stir Welding (FSW). FSW is a revolutionary solid state joining process, invented and patented by the Welding Institute, UK in the year 1991 (G.B. Patent 9125978.8, Int. Patent PCT/GB92/02203, 1991) [10]. In the FSP technique, a non-consumable tool having a shoulder and a probe of specific design is used. Probe height is kept as per targeted processing depth. Tool is rotated at certain RPM and plunged into the base metal until its shoulder is rubbing against the base metal surface. After an appropriate dwell time, the tool is then traversed along the desired processing path at definite feed rate. Due to the frictional heating caused by the tool rubbing on the base metal, the material around the tool probe softens. The combined effect of tool rotation and transverse movement results in severe plastic deformation and plastic material glide all around the tool probe [11, 12].

Amount of heat input into the base metal depends upon tool RPM and feed rate. Higher tool RPM and lower feed rate will increase the heat generated during the process. Higher heat input parameters during FSP will tend to produce coarse grain structure in the stir zone (SZ) whereas, low heat input parameters will lead to formation of tunnel defect in the SZ. Hence, optimum set of FSP parameters are required which produces fine grain defect free structure in the SZ [13]. Tool geometry also as a great impact on amount of frictional heat generation and plastic flow of material during FSP [14]. During the process, there is a chance to integrate second phase particles and create composites because of the high material flow. Therefore, to achieve both a flawless SZ and a uniform dispersion of the particles, the FSP parameters must be optimized [15].

Fabrication of surface composites (SCs) on aluminum alloy matrix using FSP technique was first exercised by Mishra et al [4]. SiC powder mixed with small amount of methanol was applied on the Al 5083 surface. FSP was performed on the preplaced SiC layer after drying in air. Tool having pin height of 1mm was used for FSP. Uniformly distributed particles having satisfactory bonding in surface Al-SiC composite layer ranging from 50 µm to 200 µm was produced by FSP technique. Increase in SC's microhardness by twice as that of base metal was reported. Since then, SC fabrication by the novel technique of FSP had motivated significant research work on this subject. Successful formation of aluminum based MMCs reinforced with particles like SiC [16-19], Al_2O_3 [20], [21], TiO_2 [22], B_4C [23-25], NiTi [26] and Si_3N_4 [27] have been reported.

Different techniques of incorporating surface MMCs by FSP have been adopted by researchers. Reinforcement particles are prefilled in groove cut or blind holes drilled on the parent metal surface [28, 29]. FSP is performed later on to mix the reinforcement with the metal matrix. Loss of reinforcement particles during FSP had been a prime concern as exact targeted proportion of reinforcement particles deposition is difficult to achieve. In order to reduce loss of reinforcement particles during FSP, they are blended with methanol before prefilling in the groove or hole and then dried in the air so that they stick together and with the metal surface during FSP being performed [4, 30]. To further reduce loss of reinforcement particles, a capping pass is performed utilizing a pinless tool before final FSP using a usual tool having a pin [24, 31]. A thin plate was used to cover the groove in a different method adopted by Mahmoud et al. [32] and Lim et al. [33]. FSP was then applied to the plate along the groove. This technique successfully avoids material loss, but it still has problems with bonding the original plate to the "cover plate", which necessitates specialized tool design and meticulous control over other process variables. To produce surface reinforcement particles on AZ31 material, Huang et al. [34] adopted a direct-FSP approach with a hollow pin-less tool pre-filled with SiC powder. SiC powder is deposited during FSP through a hollow pin-less tool carrying a centrally drilled hole of 8mm. Under the optimum process parameters of the direct-FSP, an unvarying composite layer up to depth of 150 µm was constructed.

FSP tool configuration and process parameters are the two main characteristics which can be varied to achieve homogenous particle distribution. Low axial force and lesser processing depth will not be effective in uniform dispersion of reinforcement particles whereas higher axial force for deeper processing target depth will expel

surface reinforcement particles from the surface [4, 34]. Higher tool feed rate will lead to decrease in heat input during FSP. This can result in the lack of the necessary plastic martial flow for particle dispersal. Multi pass FSP technique may therefore be adopted to improve reinforcement particle distribution [35-37]. By and large it is observed that increasing tool rotation speed and decreasing too feed rate will improve reinforcement particle dispersion [38]. Greater heat input associated with multi-pass FSP causes improved stirring and mixing [39]. Influence of tool pin geometry on reinforcement element distribution has been studied by many researchers. Mahmoud et al. [32] had studied effect of tool probe size and shape on SiC dispersion in A1050-H24 aluminum metal matrix by FSP. They have discovered that the tool having square probe had uniformly disseminated the SiC particles in the stir zone compared to other tool probe profile irrespective of tool rotation speed. However, the uniformity of the SiC particle distribution in the nugget zone was not significantly affected by the probe size. Azizieh et al. [38] had compared nanoparticle distribution using columnar probe with and without thread, and thread with three flutes by FSP method. The results of their experiments demonstrated that homogeneous nanoparticle dispersion was obtained using a tool probe with a thread without flutes. Threads promote downward motion of material flow along the thread during FSP.

In the present investigation, surface reinforcement of Al 5083 TIG butt weld surface by SiC composite fabrication via direct friction stir processing (DFSP) method is proposed. FSP tool used in this work is a hollow tool having a cylindrical pin. Homogenous dispersion of SiC particles in aluminum matrix was achieved in single pass of DFSP. This new approach is based on direct particle injection technique during performing FSP. Therefore, objective of this work is to eliminate pre-FSP operations performed on the plate surface such as groove cutting or hole drilling and achieve homogenous SiC distribution in single pass FSP.

2. MATERIAL AND METHOD

Cold rolled aluminum alloy 5083 sheet of 6mm thickness was used in this work. Weight % composition of Al 5083 according to ASTM B209/B928M is 5% Mg, 0.15% Si, 0.35% Fe, 0.05% Cr, 0.05% Cu, 0.02% Zn and rest is Al. To produce surface composite layer, commercially available SiC powder of 400 mesh size was used as reinforcement element. 75mm x 150mm size plate was cut using abrasive cutting disc and faying surface was made flat grounded to produce zero root gap setup for Tungsten Inert Gas (TIG) welding which is shown in Figure 1.

Faying surfaces and nearby region of welding was rubbed by polish paper followed by acetone cleaning to remove aluminum oxide, oil and dirt prior to TIG welding. Butt joint of Al 5083, 6mm thick plate was produced by TIG welding without adding filler wire. Welding was performed on machine welding station where torch travel was controlled by machine. Therefore, constant TIG welding torch travel speed was achieved by maintaining constant arc length. TIG welding was performed using Lincoln Electric made Aspect 300 welding machine. Welding parameters were 150 Amp current, 16 V voltage, 120 mm/min travel speed, 13-15 lpm shielding gas flow rate. Argon gas having 99.95% purity was used as shielding gas. Two autogenous TIG welding passes, one each on either side, were deposited to produce full fusion butt joint of Al 5083, 6mm thick plate.

After TIG welded plate cooled down to room temperature, it was mounted on a milling machine table for performing Direct Friction Stir Processing (DFSP) on it. Geeta Engineering Pvt. Ltd. made milling machine was used for performing DFSP. Specially designed non-consumable hollow tool was used to direct implant SiC surface composite simultaneously during performing FSP as illustrated in Figure 2. The FSP tool was manufactured from the tool steel followed by hardening (heating in the range of 840 °C to 870 °C and oil quenching) and tempering (heating in the range of 500 °C to 650 °C and oil quenching). The targeted depth for surface processing was up to 2mm. Therefore, hollow FSP tool is also having cylindrical probe of 5mm dimeter and 1.8mm length. Known quantity of SiC powder was prefilled in the hollow FSP tool. After completion of one FSP pass, remaining SiC powder was collected and weighed to get

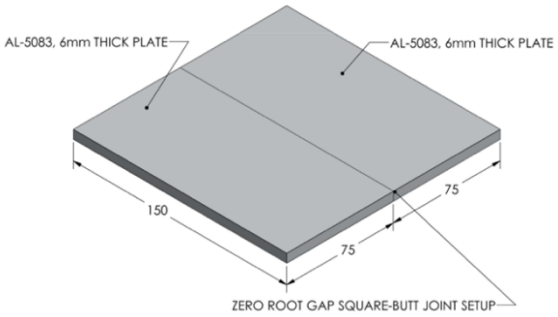

Figure 1. Square Butt Joint Set-up

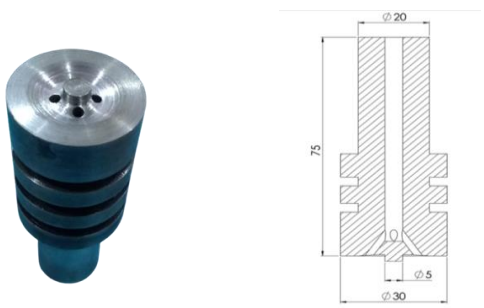

Figure 2. Hollow Tool for DFSP (Dimensions shown are in mm)

the SiC consumption value during FSP by weight difference. Weight measurement was taken on analytical balance (Ana Matrix Instrument Technologies Pvt. Ltd., HZK-FA210) having maximum capacity of 210 gm and readability 0.1 mg sensitivity. After cooling to room temperature, DFSP on other side of the plate was performed. DFSP was performed at three different tool rotational speed to find out effect of frictional heat input on the SiC particle distribution and mechanical characteristics of the weld joint. Different set of DFSP parameters are shown in Table 1.

Macro examination of weld cross section was performed to evaluate processing depth and to ensure absence of macro defects. Microstructural evaluation of Direct Friction Stir Processed (DFSPed) specimen was performed on Carl Zeiss, Jena, Model-EPY Type-2 optical microscope. Specimen for macro and micro examination was sectioned perpendicular to the weld seam and they were etched with Keller's reagent. ImageJ software was used to digitally measure the grain size (diameter).

To reveal the mechanical properties of the weld joint after performing FSP on it, tensile test and microhardness tests were performed. Sub sized specimens, according to ASTM B557 were prepared for tensile test and test was performed on computer controlled tensometer having 2 Ton load capacity. Microhardness was measured using diamond indenter by applying 200gm force for 20 seconds dwell time. Microhardness measurement was carried out starting from the weld center to going away from the weld center to cover all regions of the weldment.

Scanning Electron Microscopy (SEM) analysis of as-processed specimen on top surface and on cross-section was performed to evaluate presence and dispersion of SiC particles. EDS was used for qualitative analysis of DFSPed specimens. Chemical analysis of both TIG welded specimen and DFSPed specimen were evaluated by EDS method. SEM and EDS were performed on Hitachi made, Model - S-3400N machine. X-Ray Diffraction (XRD) scan was also performed on the DFSPed specimen to identify the crystalline phases and compound types present in the material.

3. RESULT AND DISCUSSION

3. 1. Macro and Micro Examinations

Figure 3 shows cross-sectional macrograph of Autogenous TIG welding followed by FSPed specimen. Macrograph reveals complete overlapping of both Autogenous TIG welding passes to produce full fusion weld joint. No traces of lack of fusion, macro pores, undercut and crack in the weldment were observed in the macro examination. Figure 4 shows microstructures of autogenous TIG welded plate at various locations viz. weld metal, HAZ and unaffected base metal. Due to the fact that, aluminium 5xxx series is a non-heat treatable and work hardenable alloys, the base metal microstructure is observed similar to that of rolling work hardening microstructure as shown in Figure 5(c). Microstructure of uninfluenced parent metal reveals un-recrystallized, and elongated grain in aluminum solid solution. It is evident that in case of fusion welding process such as TIG welding process, a wide HAZ arises as a result of material fusion and high temperatures experienced by nearby base material. The HAZ microstructure, as shown in Figure 5(b) reveals fine intermetallic particles distributed in coarse recrystallised grains of average grain size of 35 μm in aluminum solid solution. No cracks or porosities were observed in the HAZ region. The weld metal microstructure shows fine columnar-dendritic, epitaxial grains having average grain size of 22 μm in aluminum solid solution that has inter-dendritic eutectic constituents primarily Al_3Mg_2. The HAZ area, on the other hand, lacks columnar grain structure. Some traces of micro-pores were observed in the weld metal microstructure shown in Figure 5(a). The novel approach of using DFSP on autogenous TIG welded joint showed significant improvement in weld zone microstructure and resulted in improvement of mechanical properties. Figure 6 shows microstructures of TIG + DFSP welded joint with addition of SiC surface reinforcement particles. Microstructure reveals that previous coarse grain dendritic TIG welded structure is crushed by strong stirring effect produced by FSP tool. Temperature in the stir zone was lower than melting point of the base metal

TABLE 1. DFSP Parameters and Tensile Test Results

Sample ID	Tool RPM	Feed Rate, mm/min	UTS, MPa	% Elongation
B1	-	-	299.67	22
T1	-	-	282.5	20
TFH1	545	31.5	213.6	17
TFH2	765	31.5	227.3	18.75
TFH3	380	31.5	189.3	9.37

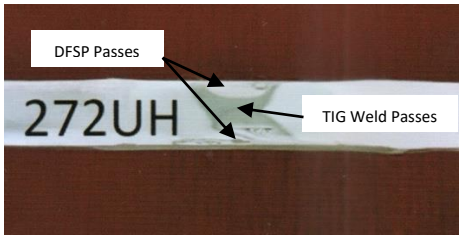

Figure 3. Macrograph of Autogenous TIG + FSP Specimen

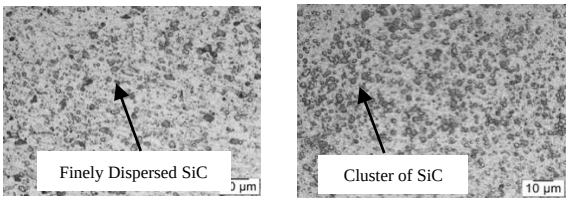

(a) DFSP at 765 RPM (b) DFSP at 545 RPM

Figure 4. Comparison of DFSP Microstructure at Tool Rotation Speed of (a) 765 rpm and (b) 545 rpm

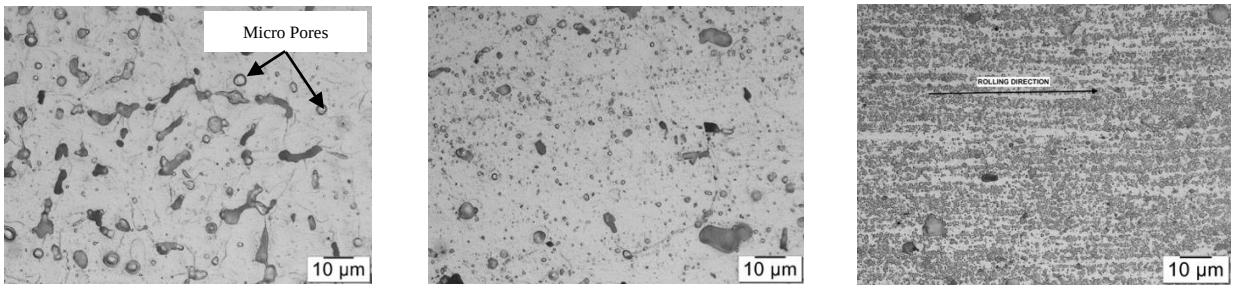

(a) TIG Weld (b) TIG HAZ (c) Base Metal

Figure 5. Autogenous TIG Weld Microstructure, Magnification 500x

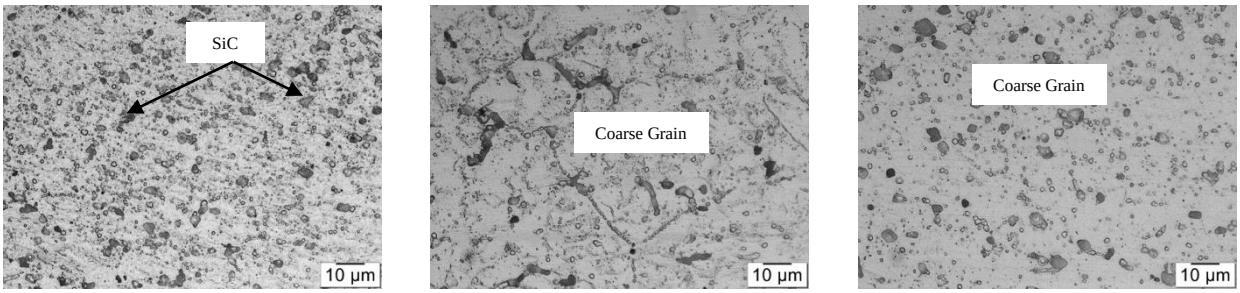

(a) At Top of Specimen FSPed Region (SiC addition) (b) At Center of Specimen TIG Weld Region (c) TMAZ

Figure 6. Autogenous TIG Weld + DFSP Microstructure, Tool Rotation at 765 RPM, Magnification 500x

but high enough to promote recrystallisation and produces fine grained equiaxed structure (average grain size of 4.6 μm) in the SZ of TIG + DFSPed specimens. Microstructural evaluation reveals fine dispersion of SiC particles (dark regions) in the fine grain crystallized structure of Aluminium solid solution. The particles were pushed and churned into the TIG weld metal as they release out of the through hole into the confined area between the incurved shoulder and workpiece during DFSP. As a result, the particles dispersed in the SZ in a homogenous and distributed manner after only single pass operation. However, dispersion of SiC particles was finer at higher tool rotation speed of 765 rpm compared to tool rotation speed of 545 rpm as shown in Figure 4. Significant amount of micro pores were seen in the microstructure of stir zone of TIG + DFSPed weldment, which resulted in drop in UTS of the weld joint. These pores are the result of hydrogen entrapment during DFSP method in which SiC powder is used to deposit on the surface of the TIG weldment. SiC powder may be the primary source of hydrogen in the weldment which is trapped during cooling of the stir zone. Comparison of microstructures of the weld center shown in Figures 5(a) and 6(b) discovers that core microstructure of unprocessed TIG weld metal of FSPed specimen shows grain growth due to added heat of FSP (average grain size of 57 μm).

Subsequent grain coarsening was also observed in the TMAZ of DFSPed specimen (average grain size of 30 μm) as shown in Figure 6(c). Figure 7 shows XRD images of TIG welded aluminum 5083 alloy (T) and SiC reinforced aluminum 5083 alloy (THF) subjected to single pass of DFSP. Clear peak of Al was seen in both the cases where as marginal peak of SiC was also observed in TIG+DFSP specimen. Since the volume fraction of Al is higher than that of SiC, SiC peaks seems to be week in Al/SiC composite. Another interesting information was revealed during XRD was no traces of γ phase ($Mg_{17}Al_{12}$) was reported in both TIG and TIG+DFSP specimens. Some researchers have discovered the formation of this phase in the weld zone of Al5XXX, however the existence of phase is not seen in our work. As γ phase ($Mg_{17}Al_{12}$) is rich in Mg and time required for diffusion of Mg is not sufficient to form this phase [40]. It is also evident from the XRD analysis that no intermetallic phases were formed after performing DFSP. SEM images of TIG welded specimen and TIG + DFSP specimens are shown in Figure 8. SEM scan of TIG weld region in the centre shows no clear indication of

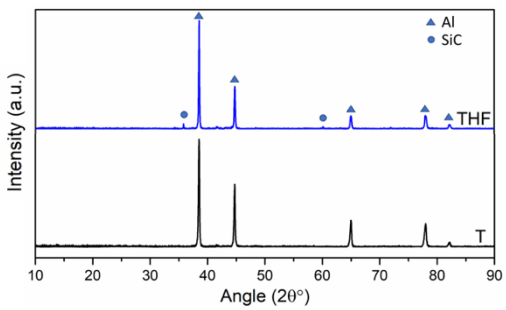

Figure 7. XRD Image of TIG + DFSP Specimen

micro pores (Figure 8b) whereas, SEM scan of SZ of DFSP at the top and at the cross section shows uniform dispersion of SiC particles in aluminum matrix. No clustering of SiC particles were observed even after single pass of DFSP (Figures 8c and 8d). Differences in size of SiC particles were observed in the SEM analysis. Extreme plastic deformation and shearing effect caused by FSP tool leads to reduction in the SiC particle size [31]. EDS result shown in Figure 8e reveals significant amount of Si and C along with parent element Al which confirms uniform distribution and presence of SiC particles in the SZ of DFSP. No sign of any detrimental inter-metallics were reported in EDS analysis of SZ of DFSPed region.

3. 2. Mechanical Properties The Ultimate Tensile Strength (UTS) of Autogenous TIG and Autogenous TIG + DFSP (Hollow Tool, addition of SiC) weld specimens are presented in Table 1. Tensile test result shows that UTS of TIG welded specimen (282.5 MPa) is 5.7% lower than base metal UTS (299.67 MPa). UTS of a specimen after depositing SiC on TIG weld through DFSP is found to be 227.3 MPa which is 19.5% lower than UTS of TIG weld. Comparing UTS values of DFSPed specimens at different tool rotation speed, better tensile strength is reported for tool rotation speed of 765 RPM whereas least tensile strength is reported for lowest tool RPM of 380 RPM. Low tool rpm is responsible for insufficient churning action of base metal for better grain refinement. Better dispersion of SiC particles in aluminium matrix can be achieved using higher tool rotation speed even in single pass [41]. Marginal loss in ductility of weld metal is observed after Autogenous TIG welding due to formation of dendritic structure and intermetallic compounds in the weld metal. However, in DFSP weld specimen, further reduction in ductility of weldment is observed due to deposition of SiC reinforcements in stir zone. HAZ damage in non-heat treatable alloys is limited

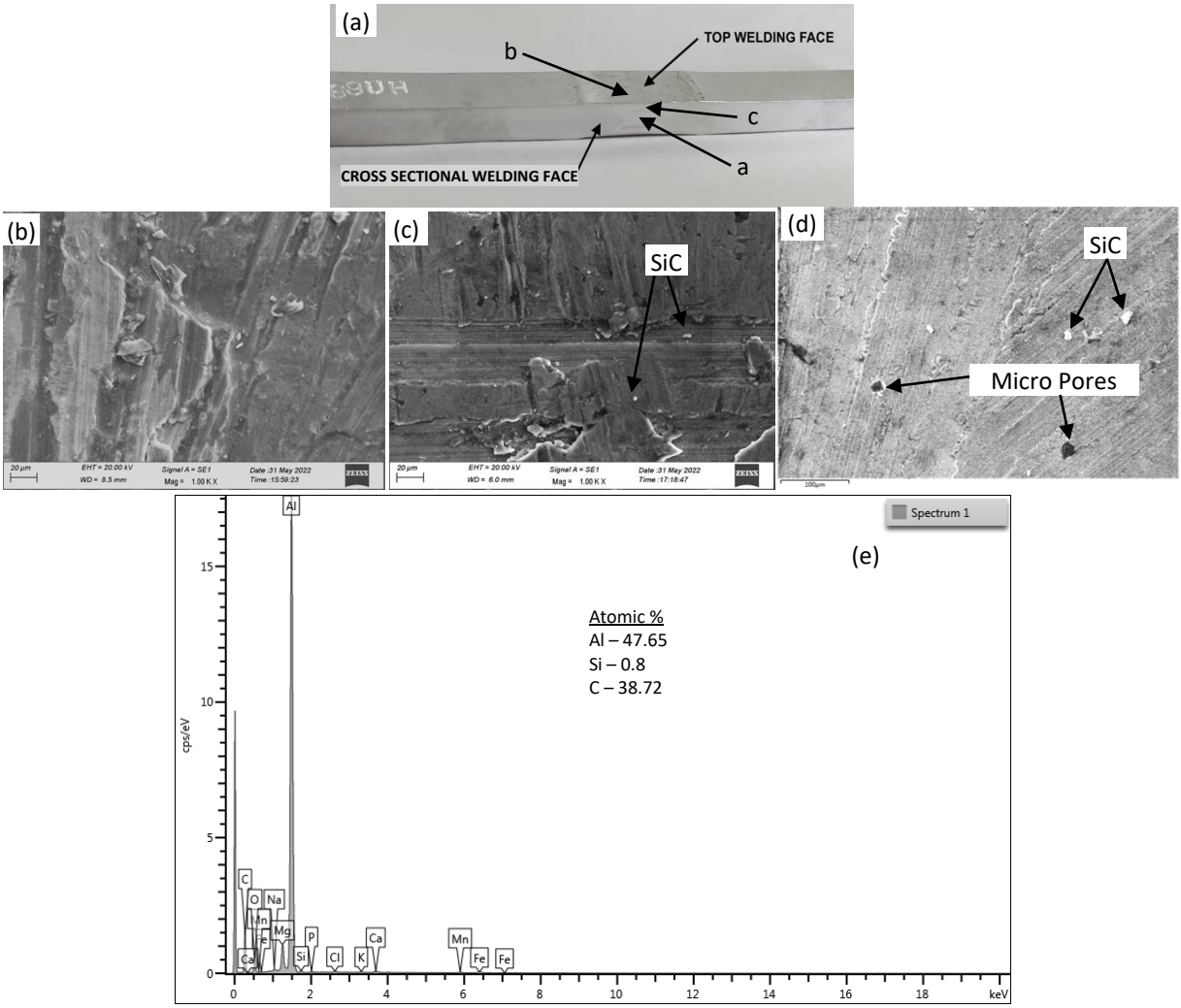

Figure 8. (a) Weld cross section macro image showing location of SEM spots; SEM Images of (b) TIG Weld at cross section; (c) SZ of DFSP at top face; (d) SZ of DFSP at cross section, (e) EDS Result of Shown Area in image C; Magnification 1000 X

to grain coarsening, recrystallization, and recovery, as opposed to heat treatable alloys, where strengthening precipitates may dissolve or coarsen. As a result, the HAZ strength loss is not nearly as severe as it is in heat treatable alloys. Dendritic microstructure of the TIG weld metal lowers tensile strength of the weld joint whereas, fine grain equiaxed microstructure in the SZ of the DFSPed region tends to increase tensile strength.

Figure 9 shows microhardness mapping of Autogenous TIG and Autogenous TIG + DFSP (Hollow Tool, addition of SiC surface reinforcement) weld specimens across the weld seam. Maximum hardness value of average 107 Hv is reported in the weld area for all the specimens. Maximum micro hardness value in the stir zone of DFSP specimen is observed due to presence of SiC particles. The results of micro hardness tests range between 80 and 110 HV, indicating softening in the HAZ region. This is mostly due to recrystallisation in the weld and HAZ that occurred during welding. The hardness of TMAZ of DFSP region reduced somewhat (average 93.3 Hv) compared to SZ because of second phase particle disintegration and coarsening produced by thermo-mechanical effect.

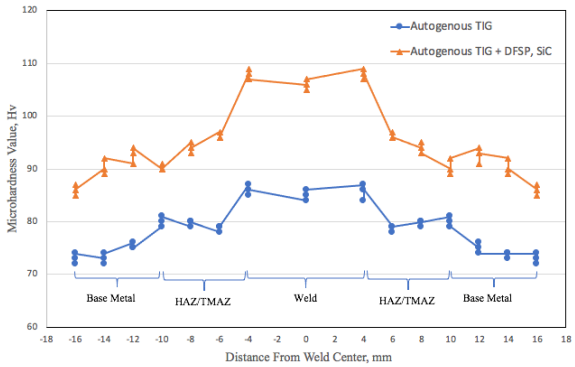

Figure 9. Microhardness Mapping of Autogenous TIG Weld and DFSP Specimen

4. CONCLUSION

Al-SiC surface composites are successfully fabricated through Direct Friction Stir Processing (DFSP) technique using hollow tool without forming any macro welding defects in stir zone. The conclusions from the test results are summarized as below:

The welding parametes, 150 Amp current, 16 V voltage, and 120 mm/min travel speed are capable of producing full fusion weld joint by autogenous TIG welding process.

Novel approach of directly depositing SiC reinforcement particles in aluminum metal metrix is successfully demonstrated by using DFSP technique with the help of hollow tool having a pin. SEM and XRD analysis confirm presence of SiC particles in SZ of DFSP. EDS scan reveals uniform dispersion of reinforcement particles even after single pass of DFSP.

Study of microstructures and SEM images reveals micro porosities in Autogenous TIG weld metal and in SZ of DFSP after depositing SiC surface reinforcement. Considerable Grain coarsening in weld metal and HAZ is observed after Autogenous TIG weld. Whereas evenly distributed SiC particles in fine grain recrystallized structure is observed in SZ of DFSP specimen.

Maximum UTS of DFSP specimen (227.3 MPa) is reported for the tool rotation speed of 765 RPM and travel speed of 31.5 mm/min. UTS of DFSPed specimen was 19.5% lower than Autogenous TIG weld UTS of 282.5 MPa. From the measurement of percentage elongation, loss of ductility of TIG weld is also reported after performing DFSP on it. However, microhardness value of SZ of DFSP is increased by 25.5% due to presence of SiC particles.

5. REFERENCES

1. Bauri, R., Ram, G.J., Yadav, D. and Kumar, C.S., "Effect of process parameters and tool geometry on fabrication of Ni particles reinforced 5083 Al composite by friction stir processing," ***Materials Today: Proceedings***, Vol. 2, No. 4-5, (2015), 3203-3211, doi: 10.1016/j.matpr.2015.07.115.
2. Sharma, D.K., Mahant, D. and Upadhyay, G., "Manufacturing of metal matrix composites: A state of review," ***Materials Today: Proceedings***, Vol. 26, (2020), 506-519, doi: 10.1016/j.matpr.2019.12.128.
3. Nguyen-Dinh, N., Hejjaji, A., Zitoune, R., Bouvet, C. and Crouzeix, L., "Nguyen-Dinh, N., et al. "Machining of FRP composites: surface quality, damage, and material integrity: critical review and analysis", ***Futuristic Composites***, Springer Singapore, (2018), 1-35.
4. Mishra, R.S., Ma, Z.Y. and Charit, I., "Friction stir processing: a novel technique for fabrication of surface composite," ***Materials Science and Engineering: A***, Vol. 341, No. 1, (2003), 307-310, doi: https://doi.org/10.1016/S0921-5093(02)00199-5.
5. Pantelis, D., Tissandier, A., Manolatos, P. and Ponthiaux, P., "Formation of wear resistant Al-SiC surface composite by laser melt-particle injection process," ***Materials Science and Technology***, Vol. 11, No. 3, (1995), 299-303, doi: 10.1179/mst.1995.11.3.299.
6. Tailor, S., Mohanty, R.M., Sharma, V.K. and Soni, P.R., "Fabrication and Wear Behavior of Nanostructured Plasma-Sprayed 6061Al-SiCp Composite Coating," ***Journal of Thermal Spray Technology***, Vol. 23, No. 7, (2014), 1081-1088, doi: 10.1007/s11666-014-0065-6.
7. Choo, S.H., Lee, S. and Kwon, S.J., "Effect of flux addition on the microstructure and hardness of TiC-reinforced ferrous surface composite layers fabricated by high-energy electron beam irradiation," ***Metallurgical and Materials Transactions A***, vol. 30, No. 12, (1999), 3131-3141, doi: 10.1007/s11661-999-0224-4.
8. Attia, A.N., "New phase reinforcement for composite materials," ***Materials & Design***, Vol. 22, No. 6, (2001), 459-466, doi: 10.1016/s0261-3069(00)00080-7.
9. Mishra, R.S., Mahoney, M.W., McFadden, S.X., Mara, N.A. and Mukherjee, A.K., "High strain rate superplasticity in a friction stir

processed 7075 Al alloy," ***Scripta Materialia***, Vol. 42, No. 2, (1999), 163-168, doi: 10.1016/S1359-6462(99)00329-2.

10. Thomas, W. M., "Friction stir welding and related friction process characteristics," Proc. 7th International Conference Joints in Aluminium (INALCO'98), *(*1998), 1-18.
11. Mehdi, H. and Mishra, R.S., "Effect of friction stir processing on mechanical properties and heat transfer of TIG welded joint of AA6061 and AA7075," ***Defence Technology***, Vol. 17, No. 10 (2021), 715-727, doi: 10.1016/j.dt.2020.04.014.
12. Mishra, R.S. and Ma, Z.Y., "Friction stir welding and processing," ***Materials Science and Engineering: R: reports***, Vol. 50, No.1, (2005), 1-78, doi: https://doi.org/10.1016/j.mser.2005.07.001.
13. Tandel, K.D. and Menghani, J.V., "Effect of Friction Stir Processing on Fusion Welded Joint of Al-5083," ***International Journal of Engineering, Transactions C: Aspects***, Vol. 35, No. 9 (2022), 1735-1743, doi: 10.5829/IJE.2022.35.09C.09.
14. Aval, H.J., "Influences of pin profile on the mechanical and microstructural behaviors in dissimilar friction stir welded AA6082--AA7075 butt Joint," ***Materials & Design***, Vol. 67, (2015), 413-421, doi: https://doi.org/10.1016/j.matdes.2014.11.055.
15. Sudhakar, M., Rao, C.S. and Saheb, K.M., "Production of Surface Composites by Friction Stir Processing-A Review," ***Materials Today: Proceedings***, Vol. 5, No. 1, Part 1, (2018), 929-935, doi: https://doi.org/10.1016/j.matpr.2017.11.167.
16. Sharma, A., Sharma, V.M., Mewar, S., Pal, S.K. and Paul, J., "Friction stir processing of Al6061-SiC-graphite hybrid surface composites," ***Materials and Manufacturing Processes***, Vol. 33, No. 7, (2018), 795-804, doi: 10.1080/10426914.2017.1401726.
17. Salehi, M., Saadatmand, M. and Mohandesi, J.A., "Optimization of process parameters for producing AA6061/SiC nanocomposites by friction stir processing," ***Transactions of Nonferrous Metals Society of China***, Vol. 22, No. 5, (2012), 1055-1063, doi: https://doi.org/10.1016/S1003-6326(11)61283-1.
18. Dolatkhah, A., Golbabaei, P., Givi, M.B. and Molaiekiya, F., "Investigating effects of process parameters on microstructural and mechanical properties of Al5052/SiC metal matrix composite fabricated via friction stir processing," ***Materials & Design***, Vol. 37, (2012), 458-464, doi: https://doi.org/10.1016/j.matdes.2011.09.035.
19. Jain, S. and Mishra, R.S., "Microstructural and mechanical behavior of micro-sized SiC particles reinforced friction stir processed/welded AA7075 and AA6061," ***Silicon***, (2022), doi: 10.1007/s12633-022-01716-5.
20. Mehdi, H., Mehmood, A., Chinchkar, A., Hashmi, A.W., Malla, C. and Mohapatra, P., "Optimization of process parameters on the mechanical properties of AA6061/Al2O3 nanocomposites fabricated by multi-pass friction stir processing," ***Materials Today: Proceedings***, Vol. 56, (2022), 1995-2003, doi: https://doi.org/10.1016/j.matpr.2021.11.333.
21. Kianezhad, M. and Raouf, A.H., "Effect of nano-Al2O3 particles and friction stir processing on 5083 TIG welding properties," ***Journal of Materials Processing Technology***, Vol. 263, (2019), 356-365, doi: https://doi.org/10.1016/j.jmatprotec.2018.08.010.
22. Khodabakhshi, F., Simchi, A., Kokabi, A.H., Nosko, M., Simanĉik, F. and Švec, P., "Microstructure and texture development during friction stir processing of Al-Mg alloy sheets with TiO2 nanoparticles," ***Materials Science and Engineering: A***, Vol. 605, (2014), 108-118, doi: 10.1016/j.msea.2014.03.008.
23. Rejil, C.M., Dinaharan, I., Vijay, S.J. and Murugan, N., "Microstructure and sliding wear behavior of AA6360/(TiC+B 4C) hybrid surface composite layer synthesized by friction stir processing on aluminum substrate," ***Materials Science and Engineering: A***, Vol. 552, (2012), 336-344, doi: 10.1016/j.msea.2012.05.049.
24. Rana, H.G., Badheka, V.J. and Kumar, A., "Fabrication of Al7075/B4C surface composite by novel Friction Stir Processing (FSP) and investigation on wear properties," ***Procedia Technology***, Vol. 23, (2016), 519-528.
25. Boopathi, S., Thillaivanan, A., Pandian, M., Subbiah, R. and Shanmugam, P., "Friction stir processing of boron carbide reinforced aluminium surface (Al-B4C) composite: Mechanical characteristics analysis," ***Materials Today: Proceedings***, Vol. 50, (2022), 2430-2435, doi: https://doi.org/10.1016/j.matpr.2021.10.261.
26. Dixit, M., Newkirk, J.W. and Mishra, R.S., "Properties of friction stir-processed Al 1100-NiTi composite," ***Scripta Materialia***, Vol. 56, No. 6, (2007), 541-544, doi: 10.1016/j.scriptamat.2006.11.006.
27. Moghaddas, M.A. and Kashani-Bozorg, S.F., "Effects of thermal conditions on microstructure in nanocomposite of Al/Si 3N 4 produced by friction stir processing," ***Materials Science and Engineering: A***, Vol. 559, (2013), 187-193, doi: 10.1016/j.msea.2012.08.073.
28. Akinlabi, E.T., Mahamood, R.M., Akinlabi, S.A. and Ogunmuyiwa, E., "Processing parameters influence on wear resistance behaviour of friction stir processed Al-TiC composites," ***Advances in Materials Science and Engineering***, (2014).
29. Akramifard, H.R., Shamanian, M., Sabbaghian, M. and Esmailzadeh, M., "Microstructure and mechanical properties of Cu/SiC metal matrix composite fabricated via friction stir processing," ***Materials & Design***, Vol. 54, (2014), 838-844, doi: https://doi.org/10.1016/j.matdes.2013.08.107.
30. Mazaheri, Y., Karimzadeh, F. and Enayati, M.H., "A novel technique for development of A356/Al2O3 surface nanocomposite by friction stir processing," ***Journal of Materials Processing Technology***, Vol. 211, No. 10, (2011), 1614-1619, doi: 10.1016/j.jmatprotec.2011.04.015.
31. Rathee, S., Maheshwari, S., Siddiquee, A.N. and Srivastava, M., "Distribution of reinforcement particles in surface composite fabrication via friction stir processing: Suitable strategy," ***Materials and Manufacturing Processes***, Vol. 33, No. 3, (2018), 262-269, doi: 10.1080/10426914.2017.1303147.
32. Mahmoud, E.R.I., Takahashi, M., Shibayanagi, T. and Ikeuchi, K., "Effect of friction stir processing tool probe on fabrication of SiC particle reinforced composite on aluminium surface," ***Science and Technology of Welding and Joining***, Vol. 14, No. 5, (2009), 413-425, doi: 10.1179/136217109X406974.
33. Lim, D.K., Shibayanagi, T. and Gerlich, A.P., "Synthesis of multi-walled CNT reinforced aluminium alloy composite via friction stir processing," ***Materials Science and Engineering: A***, Vol. 507, No. 1-2, (2009), 194-199, doi: 10.1016/j.msea.2008.11.067.
34. Huang, Y., Wang, T., Guo, W., Wan, L. and Lv, S., "Microstructure and surface mechanical property of AZ31 Mg/SiCp surface composite fabricated by Direct Friction Stir Processing," ***Materials & Design***, Vol. 59, (2014), 274-278, doi: https://doi.org/10.1016/j.matdes.2014.02.067.
35. Mahmoud, E.R.I., Ikeuchi, K. and Takahashi, M., "Fabrication of SiC particle reinforced composite on aluminium surface by friction stir processing," ***Science and Technology of Welding and Joining***, Vol. 13, No. 7, (2008), 607-618, doi: 10.1179/136217108X333327.
36. Yang, R., Zhang, Z., Zhao, Y., Chen, G., Guo, Y., Liu, M. and Zhang, J., "Effect of multi-pass friction stir processing on microstructure and mechanical properties of Al3Ti/A356 composites," ***Materials Characterization***, Vol. 106, (2015), 62-69, doi: 10.1016/j.matchar.2015.05.019.
37. Surekha, K., Murty, B.S. and Rao, K.P., "Microstructural characterization and corrosion behavior of multipass friction stir processed AA2219 aluminium alloy," ***Surface and Coatings Technology***, Vol. 202, No. 17, (2008), 4057-4068, doi: 10.1016/j.surfcoat.2008.02.001.

38. Azizieh, M., Kokabi, A.H. and Abachi, P., "Effect of rotational speed and probe profile on microstructure and hardness of AZ31/Al_2O_3 nanocomposites fabricated by friction stir processing," ***Materials & Design***, Vol. 32, No. 4, (2011), 2034-2041, doi: 10.1016/j.matdes.2010.11.055.

39. Sharma, V., Gupta, Y., Kumar, B.M. and Prakash, U., "Friction Stir Processing Strategies for Uniform Distribution of Reinforcement in a Surface Composite," ***Materials and Manufacturing Processes***, Vol. 31, No. 10, (2016), 1384-1392, doi: 10.1080/10426914.2015.1103869.

40. Heirani, F., Abbasi, A. and Ardestani, M., "Effects of processing parameters on microstructure and mechanical behaviors of underwater friction stir welding of Al5083 alloy," ***Journal of Manufacturing Processes***, Vol. 25, (2017), 77-84, doi: https://doi.org/10.1016/j.jmapro.2016.11.002.

41. Singh, R., Rizvi, S.A. and Tewari, S.P., "Effect of friction stir welding on the tensile properties of aa6063 under different conditions," ***International Journal of Engineering, Transactions A: Basics***, Vol. 30, No. 4, (2017), 597-603, doi: 10.5829/idosi.ije.2017.30.04a.19.

Persian Abstract

چکیده

برای ایجاد ذرات تقویت کننده سطح در ماتریس فلزی، پردازش اغتشاشی اصطکاکی اغلب مورد استفاده قرار می گیرد. تشکیل کامپوزیت سطح آلومینیوم/SiC بر روی گاز خنثی تنگستن (TIG) جوش لب به لب Al5083 توسط یک تکنیک جدید پردازش اغتشاش اصطکاکی مستقیم (DFSP) با استفاده از یک ابزار توخالی با موفقیت در این کار نشان داده شده است. رسوب SiC در منطقه اغتشاشی DFSP با روش پراش اشعه ایکس (XRD) تایید شد. تجزیه و تحلیل میکرو اتصال جوش با استفاده از میکروسکوپ متالوگرافی و میکروسکوپ الکترونی روبشی (SEM) به دست آمد. ریزساختار منطقه هم‌زن DFSP ذرات تقویت‌کننده SiC ریز توزیع شده را در ماتریس آلومینیوم نشان می‌دهد. عدم وجود مواد بین فلزی مضر با تجزیه و تحلیل طیف‌سنجی پراکنده انرژی (EDS) تایید شد. استحکام کششی نمونه DFSPed 227.3 مگاپاسکال است که ۱۹.۵٪ کمتر از UTS نمونه جوش TIG خودزا است. ریزسختی SZ از DFSP به دلیل وجود ذرات SiC از ریزسختی جوش TIG 86 Hv به ۱۰۷ Hv افزایش یافته است.